

Towards Robust Deep Neural Networks

Timothy E. Wang
United Technologies
Research Center
wangte@utrc.utc.com

Yiming Gu*
Uber
yiming.guu@gmail.com

Dhagash Mehta
United Technologies
Research Center
dhagashbmehta@gmail.com

Xiaojun Zhao
United Technologies
Research Center
zhaox@utc.utrc.com

Edgar A. Bernal†
University of Rochester
edgar.bernal@rochester.edu

Abstract

We investigate the topics of sensitivity and robustness in feedforward and convolutional neural networks. Combining energy landscape techniques developed in computational chemistry with tools drawn from formal methods, we produce empirical evidence indicating that networks corresponding to lower-lying minima in the optimization landscape of the learning objective tend to be more robust. The robustness estimate used is the inverse of a proposed sensitivity measure, which we define as the volume of an over-approximation of the reachable set of network outputs under all additive l_∞ -bounded perturbations on the input data. We present a novel loss function which includes a sensitivity term in addition to the traditional task-oriented and regularization terms. In our experiments on standard machine learning and computer vision datasets, we show that the proposed loss function leads to networks which reliably optimize the robustness measure as well as other related metrics of adversarial robustness without significant degradation in the classification error. Experimental results indicate that the proposed method outperforms state-of-the-art sensitivity-based learning approaches with regards to robustness to adversarial attacks. We also show that although the introduced framework does not explicitly enforce an adversarial loss, it achieves competitive overall performance relative to methods that do.

1. Introduction

The advent of machine learning techniques, most notably deep learning [4], has made it possible to automate

complex tasks such as vision-based object detection, natural language processing, machine translation, and stock-market analysis. Despite its tremendous success in many academic endeavors and commercial applications, the adoption of deep learning in the perception, decision and control loops of mission/safety-critical systems has been limited. One possible reason for the slow rate of adoption is the limited theoretical understanding of the inner workings of deep neural networks (DNNs). Another possible reason is the lack of guarantees of certain behavioral, and, in particular, robustness properties. One such robustness property is the ability of the network to be resistant to adversarial attacks. In an adversarial attack, the input data is perturbed minimally such that, while the resulting adversarial example closely resembles the unmolested sample, the output of the trained network is affected. Recent work in the deep learning literature [13, 28, 36, 22, 16, 34, 11] has shown that DNNs may be susceptible to adversarial examples. For state-of-art DNN image classifiers, researchers have concocted methods to reliably engineer small perturbations that result in successful adversarial examples. In one such example [13], the generated adversarial example looks, to the naked human eye, indistinguishable from the original sample, but produces a drastically different classifier output. Some input perturbations are synthetic [13], while others target physical, real-world objects [22, 11].

In traditional verification and validation (V&V) processes for safety-critical systems, the robustness of the system is assured via an extensive testing procedure which samples the expected variations in the values of the parameters of the operating environment and system inputs until certain criteria of appropriate coverage metrics are reached. This test-based approach is likely to be less effective for systems with deep learning components since the dimensions of their input spaces are typically much larger. Furthermore,

*Work carried out while at UTRC

†Work carried out while at UTRC

the lack of understanding of the topology of the input spaces involved leads to an open theoretical question: how do we define coverage metrics for V&V tests applied to systems with deep learning components? Nevertheless, we know that it is feasible to provide formal guarantees of robustness properties of small to medium DNNs [18] as well as to enforce the guarantee of a robustness property through the training process for larger DNNs [21]. With the increase in predictability that comes with the formal guarantees of adversarial robustness, it is conceivable that deep learning systems could be deployed in mission and/or safety-critical systems.

In this paper, we present a new learning framework that results in networks which are less sensitive to changes in the input, and, consequently, likely to be more robust to adversarial attacks. The method reliably yields networks of increased robustness by introducing a cost term that penalizes output sensitivity to changes in the input.

The sensitivity measure is described briefly below and is further detailed in Sec. 3. Consider a portion of a two-dimensional output space illustrated in Fig. 1 (left) where a segment of the decision boundary between classes C_1 and C_2 lies. The black dot represents the network output for a sample x belonging to C_1 . Consider a set Δ containing all possible perturbation vectors expected upon network deployment. These could include, in the case of a vision-based object classification application, synthetic noise, physical perturbations, shadows, glare, etc. Consider the input data x , and the set \mathcal{X} resulting from perturbing x with all possible disturbances from Δ . The DNN maps the perturbed input set \mathcal{X} into some output reachable set, an over-approximation of which is represented by the box in the figure. We measure the *sensitivity* of the network as the aggregate volume of all over-approximations of the output reachable set across the training samples for a pre-determined Δ .

Also shown in Fig. 1 (left) is the region of potential counter-examples (red portion of the box), which contains all the points in the over-approximated output set for which the classification changes from C_1 to C_2 , i.e., potential outputs of adversarial inputs. We hypothesize that, by reducing the volume of the output reachable set for some given perturbed input set, the possibility of successful adversarial inputs can be ameliorated, as indicated by the smaller orange box in Fig. 1 (right).

The main contributions of this paper can be summarized as follows:

- We propose a novel sensitivity metric for feedforward neural networks and introduce two different approaches to estimate it (see Sec. 3): one based on Reluplex [18], an update on the classical Simplex method that enables support of ReLU constraints; and one based on evaluating the dual cost of a Linear Programming (LP) relaxation



Figure 1: Reducing the size of the output reachable set could lead to increased robustness to adversarial inputs

of the exact encoding of the input-output mapping of a ReLU-based network [21, 9].

- We conduct an empirical study on the relationship between the sensitivities of neural networks and the energy values of their corresponding optimization landscape minima, from which we conclude that networks corresponding to lower-lying minima tend to be less sensitive than those corresponding to higher-valued minima. We also show that traditional optimization approaches based on Stochastic Gradient Descent (SGD) algorithms and regularization do not necessarily lead to networks with good sensitivity properties (see Sec. 4).
- Based on the above results, we propose a novel loss function which enables effective task-oriented learning while penalizing high network sensitivity to changes in the input (see Sec. 5). We empirically verify the effectiveness of the proposed cost function, and compare the performance of our method with that of state-of-art approaches (see Sec. 6).

2. Background and Related Work

Many supervised machine and deep learning algorithms operate based on the principle of Empirical Risk Minimization (ERM), whereby the expectation of a loss function associated with a given hypothesis is approximated with its empirical estimate. The main implication of this modus operandi is the so-called Generalization Error (GE), which refers to the difference between the empirical error and the expected error; practically speaking, the GE manifests itself in a difference in algorithm performance on unseen data relative to the performance observed on the training data. Since ERM is an optimistically biased estimation process [42], techniques to bridge (and understand) the gap between the empirical risk and the true risk have been proposed: the narrower the gap, the better the generalization properties of the algorithm. Broadly speaking, these techniques fall under one of the following categories:

2.1. Sensitivity and Robustness Analysis and Optimization

The authors of [42] define robustness as the property of a machine learning algorithm to produce similar test and

training errors when the test and training samples are similar to each other, and hypothesize that a weak measure of robustness is both sufficient and necessary for good generalizability. Furthermore, they derive a generalization bound that holds under certain constraints. The authors of [26] conclude empirically that trained neural networks are more robust to input perturbations in the vicinity of the training manifold and that higher robustness correlates well with good generalization properties. In [33], the relation between the GE and the classification margin of a neural network is studied. The authors conclude that a necessary condition for good generalization is for the Jacobian matrix of the network to have a bounded spectral norm in the neighborhood of the training samples, in line with the results presented in [26, 43, 17].

2.2. Robustness Against Adversarial Attacks

Adversarial examples are data samples constructed by applying perturbations to known training samples along directions that result in the largest change at the network output [14], so that the perturbed input, often indistinguishable from the original input, leads to an erroneous decision by the network. This vulnerability is directly related to the GE and can be ameliorated by training with adversarial examples [14]. The approach introduced in [15] aims at achieving robustness against adversarial attacks, and consists of stacking a denoising auto encoder (DAE) with the network of interest, the role of the DAE being to map back the adversarial example to the training manifold. An alternative architecture based on contractive auto encoders (CAE) is also proposed. The authors of [21] propose a method to train deep networks based on ReLU activation units that are provably robust to adversarial attacks; they achieve this by minimizing the worst-case loss across the a convex over-approximation of the reachable set under norm-bounded input perturbations.

2.3. Formal Verification of Neural Networks

Often, the GE includes behavior that is not only incorrect, but also unpredictable, which prevents deployment of deep learning algorithms in safety-critical applications. Formal verification refers to techniques aimed at providing mathematical guarantees about the behavior of systems including computer programs [29]. Formal verification is used most often for safety-critical applications in sectors such as aerospace, nuclear and rail. Early approaches to formally verifying neural networks leveraged SMT solvers [30], but did not scale well and were practical on very small networks with a single hidden layer and a small number of neurons. Reluplex [18] extended the simplex algorithm to support the piece-wise linear nature of ReLU activation units, and showed improved scalability properties. More recently, authors have tackled the prob-

lem using optimization-based approaches including: Mixed Integer Programming (MIP) formulations [6] with local search [8], LP relaxation [10], branch and bound [10, 5], and dual formulations [9, 21]. In contrast to most of the other literature, the framework introduced in [9] applies to a general class of activation functions.

2.4. Analysis of Optimization Landscapes

The training of modern machine learning models, most notably of deep networks, is posed in the form of highly non-convex optimization tasks with multiple local minima. The simplest way to quantify the quality of landscape minima is to measure their distance to the global minimum: the closer the energy of a local minimum to that of the global minimum, the better the quality of the minimum and its corresponding network. This definition is ill-posed as in general the global minimum is not known for a typical nonlinear optimization function. One of the dominant explanations as to why deep learning works so well is that there may be no bad minima at all for the loss functions of deep network [2, 32, 25, 12, 35, 7]: under certain unrealistic assumptions, it has been shown that all the local minima are global minima [19]. In more realistic scenarios, cost functions with a non-vanishing l_2 -regularization term have been shown to have local minima which are not global minima [23, 37]. Another branch of research leverages optimization methods developed for chemical physics, called the potential energy landscape theory [40]. Using such techniques, the authors of [3] showed that the landscape of the loss function for a specific feed-forward artificial neural network with one hidden layer trained on the MNIST dataset exhibited a single funnel structure. In a recent paper [24] (see also, [41, 20]), the measure of the goodness of a minimum is refined by adding further metrics in addition to the value of the cost function or the performance. The work concluded that when an overspecified artificial neural network with one hidden layer and l_2 -regularization was used to learn the exclusive OR (XOR) function, although the classification error was often zero for various minima, the sparsity structure of the network varied with the minima.

3. Measure of Robustness via Sensitivity Analysis

This section provides a detailed description of the sensitivity measure overviewed in Sec. 1, as well as of the methods that we use to estimate sensitivity for feedforward neural networks with ReLU activation nodes under l_∞ -norm bounded perturbations. Throughout the paper, we use ReLU as the activation function. A feedforward neural network is a parameterized function f_W which maps input data x_i in \mathbb{R}^n to output vectors y_i in \mathbb{R}^m . By applying l_∞ -norm bounded perturbations to an input data vector x_i , we obtain a perturbed input set $\mathcal{X} = \{x|x \in \mathbb{R}^n, \|x - x_i\|_\infty \leq \epsilon\}$,

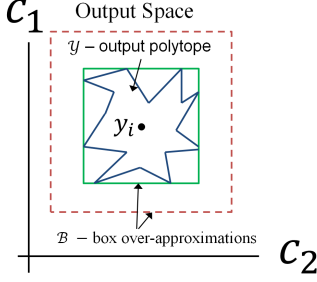


Figure 2: Proposed sensitivity measure is the volume of the box over-approximation of the output polytope which results from l_∞ -norm bounded perturbations to the input.

where ϵ denotes the perturbation bound. Given the perturbed input set \mathcal{X} , the output reachable set of the network is $\mathcal{Y} = \{y \in \mathbb{R}^m | y = f_W(x) \wedge x \in \mathcal{X}\}$. As stated earlier, we use an estimate of the volume of \mathcal{Y} as a surrogate metric for network sensitivity. For feedforward networks with ReLU activation nodes, \mathcal{Y} is generally a non-convex polytope whose exact volume is difficult to compute. Instead, we define the sensitivity of the network as the volume of a box over-approximation of the output reachable set as illustrated in Fig. 2. The over-approximation can be either tight (green box with solid boundary in Fig. 2) or loose (red box with dashed boundary in Fig. 2) depending on the computational methods used. There is a significant trade-off between the conservatism of the over-approximation and the time it takes to compute it. We now describe the two methods used in our experiments. The first method, based on the dual formulation, is used to compute a conservative (i.e., loose) over-approximation. This method turned out to be efficient enough in practice to be incorporated in the training process described in Sec. 5. The second method uses Reluplex, a SMT solver specialized for DNNs, to compute a tight over-approximation of the output polytope.

3.1. Computing Sensitivity Using a Dual Formulation

The volume of the tight over-approximation (green box in Fig. 2) can be computed by finding the min and max values along each dimension of the output vector and then computing the product of the lengths of the resulting intervals across all dimensions. Finding the min and max of the output dimensions of a N -layer ReLU network requires solving a set of difficult optimization problems i.e., minimize and maximize $y[i]$, $i = 1, \dots, m$, where $y[i]$ is the i -th entry of the output vector y , subject to a set of piece-wise linear constraints imposed by the ReLU activations. The min of $y[i]$ (denoted $y_{min}[i]$) under l_∞ -norm bounded perturbations to input x with bound ϵ is the solution of the

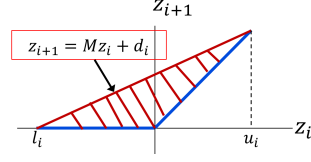


Figure 3: Linear relaxation of piece-wise linear constraints.

following set of optimization problems:

$$\text{minimize } y[i], \quad i = 1, \dots, m \quad (1)$$

$$\text{subject to } x[j] - \epsilon \leq \hat{x}[j] \leq x[j] + \epsilon, \quad j = 1, \dots, n \quad (2)$$

$$z_1 = W_0 \hat{x} + b_0 \quad (3)$$

$$y = W_N z_N + b_N$$

$$z_{k+1} = \max(0, W_k z_k + b_k), \quad k = 1, \dots, N-1 \quad (4)$$

where N is the number of layers in the network, and W_k and b_k are the weights and biases between layers k and $k+1$, respectively. The constraints in Eq. 2 capture the fact that the input belongs to the perturbed set \mathcal{X} . The piece-wise linear constraints in Eq. 4 denote the relations between the inputs and outputs of the layers with ReLU activations. The max of $y[i]$ (denoted $y_{max}[i]$) is just the negative of the min of $-y[i]$ in Eq. 1. The volume of the over-approximation is:

$$\prod_{i=1}^m y_{max}[i] - y_{min}[i] \quad (5)$$

It is known within the operational research community that the optimization problem in 1 can be transformed into a mixed-integer linear programming (MILP) problem through the usage of the big- M trick [31]. Therefore computing the sensitivity of a network can be done by solving a MILP using a state-of-art solver such as Gurobi [27] or by using other techniques with exact encodings benchmarked in recent work [5]. However, it remains difficult to scale up the “exact” methods to efficiently verify sensitivity of networks with multiple fully-connected layers and more than hundreds of ReLU nodes.

Due to the associated computational complexity, using methods with exact encodings is not yet practical for our main goal, which is to incorporate the sensitivity measure into the loss function driving the learning. Instead, we adopt an approach inspired by recent work in which ReLU constraints are relaxed into a set of linear constraints. The relaxation is illustrated graphically in Fig. 3. Consider the piece-wise linear constraints $z_{i+1} = \max(0, W_i z_i + b_i)$ from Eq. 4; under the relaxation procedure, they are trans-

formed into a set of linear constraints:

$$\begin{aligned} z_{i+1} &\leq Mz_i + d_i \\ l_i &\leq z_i \leq u_i \\ z_{i+1} &\geq z_i \\ z_{i+1} &\geq 0 \end{aligned} \quad (6)$$

With the linear constraints in Eq. 6, the optimization task in Eq. 1 is transformed into a primal linear programming (LP) problem. Furthermore, the dual objective, when evaluated at any feasible point, becomes a lower-bound to the primal objective. As noted in [21], there is a feasible point which can guarantee in practice a “sufficiently tight enough” lower bound to the primal objective.

Let $J(x, C, \epsilon, \nu; W)$ be the dual objective function from [21], where x is the input data, C is the primal objective matrix, ϵ is the l_∞ norm bound of the allowable input perturbations, ν is the dual variable, and W represents the network parameters; the *sensitivity function* $S(x, \epsilon, \nu; W)$, which measures the sensitivity of a neural network under norm-bounded perturbations, is given by:

$$S(x, \epsilon, \nu; W) = \prod_{j=1}^m \frac{-J(x, -I_{m \times m}, \epsilon, \nu; W)[j]}{-J(x, I_{m \times m}, \epsilon, \nu; W)[j]} \quad (7)$$

where $I_{m \times m} \in \mathbb{R}^{m \times m}$ is the identity matrix. Eq. 7 is the volume of a (box) over-approximation of the output reachable set of a feed-forward neural network with ReLU activation nodes under l_∞ -norm bounded perturbations with bound ϵ .

The sensitivity function can be evaluated very efficiently on a GPU-enabled laptop with CUDA for networks with multiple layers, and up to a few thousand nodes. Comparatively, the sensitivity of a similar-sized network when evaluated with an “exact method” such as Reluplex can take hours to compute. However, this computational speed advantage comes at the cost of over-estimation of the sensitivity measure, as both the linear relaxation in Eq. 6 and the evaluation of the dual objective at a feasible point adds to the conservatism of the (box) over-approximation.

3.2. Computing Sensitivity Using Reluplex

As mentioned in Sec. 3.1, several “exact” techniques benchmarked in [5] can be used to compute the volume of the tight over-approximation. In the experiments of Sec. 4, we used Reluplex as the solver. To compute the volume of the tight (box) over-approximation, we queried Reluplex the following satisfiability problem: for a given data input x and perturbation bound ϵ , does there exist a solution y that satisfies the set of constraints

$$y[i] \leq a[i] \wedge y[i] \geq b[i], i = 1, \dots, m \quad (8)$$

and Eqs. 2, 3 and 4 in which $a[i] \in \mathbb{R}$ and $b[i] \in \mathbb{R}$ are respectively the candidate min and max of $y[i]$. If Reluplex returns a negative answer, then $a[i]$ and $b[i]$ are valid lower and upper bounds to $y[i]$. Reluplex is queried repeatedly with a sequence of min and max candidates $\{a[i]_j\}$ and $\{b[i]_j\}$ until a numerical tolerance is reached. We implemented a simple bisection algorithm to generate a sequence of min and max candidates $\{a[i]_j\}$ and $\{b[i]_j\}$, and a translational tool-chain to repeatedly query Reluplex. Fig. 4 plots $\frac{S_{dual} - S_{Reluplex}}{S_{Reluplex}}$ for close to 200 networks (each corresponding to different landscape minima) in which S_{dual} is the sensitivity computed using the dual formulation and $S_{Reluplex}$ is the sensitivity computed by Reluplex on the same network with the same input perturbation bound. The large peak around network #50 shows that the dual of LP technique can occasionally over-estimate the sensitivity of a network by a large amount when compared against Reluplex, but the plot also shows that for the majority of the networks the over-estimation remains relatively insignificant.

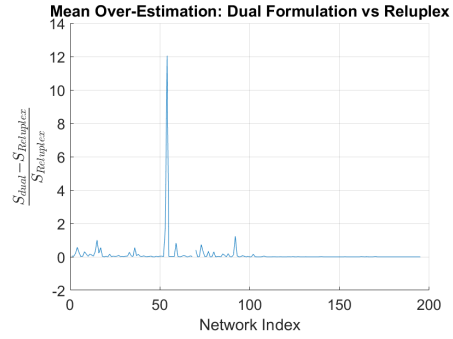


Figure 4: Relative difference between sensitivity estimation via the Dual Formulation and Reluplex.

4. Optimization Landscape Minima: Energy Value vs. Sensitivity

In this section, we investigate the quality of the different minima in the optimization landscape of neural networks by leveraging a combination of energy landscape approaches developed by chemical physicists, and the formal verification tool Reluplex developed by the computer scientists.

4.1. Computing the Minima

To find multiple minima, we use methods developed in computational chemistry to explore energy landscapes of atomic and molecular clusters, as described in [39]. First, using different quasi-Newton methods such as limited memory Broyden-Fletcher-Goldfarb-Shanno (LBFGS) and basin-hopping methods starting from different random initial guesses, we find multiple local min-

ima. Next, an eigen-vector following method is used to find multiple saddle points of index 1 again by feeding different random initial guesses and following the search in the restricted directions where the Hessian matrix has exactly one negative eigenvalue. Then, from each saddle point of index 1, we compute two steepest descent paths in two different directions to connect the corresponding pair of minima. While following this process of connecting pairs of minima, whenever any of the two end-points of this path is not in the existing database of the minima, it gets added to the database. This process is iterated a few times to obtain multiple minima, while retaining only energetically distinct minima (minima which are at different geometrical locations but have the same energy value are discrete-symmetrically related with each other and can be obtained via a discrete transformation of weights). To run these computations, we use a wrapper around Python Energy Landscape Explorer (PELE) [1], which performs energy landscape related computations (i.e., all the aforementioned steps) for any given unconstrained multivariate cost function with continuous variables, as well as Theano [38], which computes the cost function values for the given neural network architecture. To circumvent the discontinuities associated with the ReLU activation functions, we take a constant value whenever the Hessian is singular by using Theano’s built-in gradients libraries. For the Iris data, we fix the l_2 regularization parameter to 0.001. Since this is a stochastic method, there is no guarantee that all minima will be found. We only sample the minima to obtain a qualitative picture.

4.2. Iris Results and Discussion

The network architecture selected to tackle classification on the Iris dataset consists of 3 fully-connected hidden layers of 25 neurons each. We used the energy landscape methods described in Sec. 4.1 to obtain 763 Iris minima of varying energy values. The computation took a total of 20 hours on a standard laptop with a single CPU and 8GB of memory.

We measure the sensitivity of each of the networks corresponding to these minima by assuming a vector of perturbation bounds $\epsilon_v = \sigma \hat{d}$ where $\sigma = 0.05, 0.1, 0.2$, where \hat{d} is a vector containing the ranges of values of features of the entire Iris dataset; that is, the perturbation bound for each input dimension is proportional to the spread of the input data along that dimension. Given a fixed ϵ_v and an input data point x , we queried Reluplex iteratively, as described in Sec. 3.2, until convergence to the min and max of each output dimension $y[i], i = 1, 2, 3$ is achieved up to some numerical tolerance. The sensitivity of the network output is plotted as a function of the energy value of the landscape minima for $\sigma = 10\%$ in Fig. 5. It can be seen that there is a tendency for networks corresponding to lower energy minima to have lower sensitivity and hence possibly exhibit

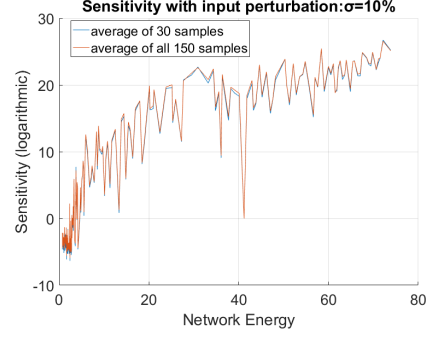


Figure 5: Network sensitivity vs. network energy for Iris landscape

more robustness to norm-bounded input perturbations. The plot illustrates the behavior of the average sensitivity for 30 samples and for all samples (150) of the Iris dataset.

5. Learning with Sensitivity Minimization

Having shown empirically that low-lying landscape minima lead to networks that are less sensitive than networks with higher energy, we now describe a new training method that encourages convergence to networks with reduced sensitivity. First, we point out that the traditional task-centric loss function (e.g., cross-entropy) plus an l_2 -regularization term does not necessarily guarantee convergence to network with reduced sensitivity. Fig. 6 shows example training runs done on the Iris dataset. The y -axis is the sensitivity of the network, and x -axis is the training epoch. It can be seen that the change in sensitivity is irregular and without any clear pattern or trend.

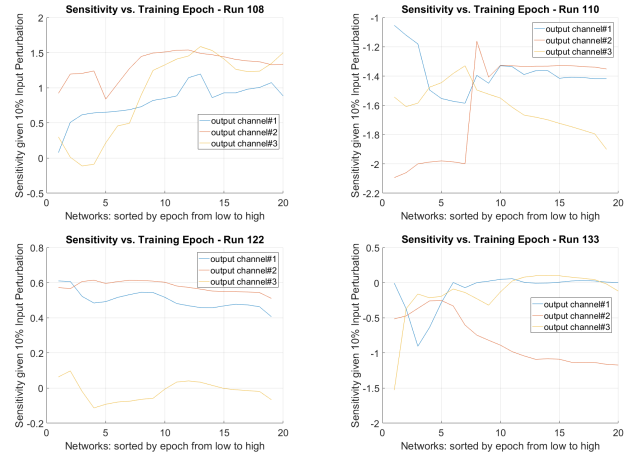


Figure 6: Samples of training runs with undesired evolution of network sensitivity.

The proposed learning framework, which aims to minimize the sensitivity of its output networks, is illustrated in

Fig. 7. The main idea of the proposed framework is to aug-

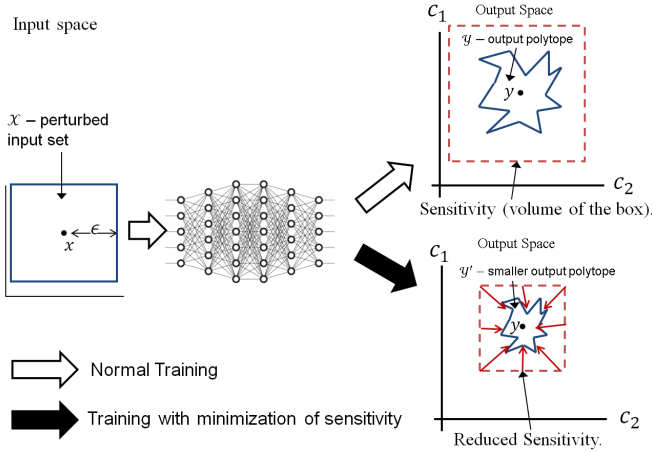


Figure 7: Proposed training method to reduce network sensitivity.

ment the usual loss function L with an additional weighted term $\lambda S(x_i, \epsilon, \nu; W)$ in which the multiplier $\lambda > 0$ is a new hyperparameter, and $S(x_i, \epsilon, \nu; W)$ is the sensitivity function from 7. Let $L(x_i, y_i; W)$ be the usual loss function with regularization incorporated. Given training sets of size M , the optimization task is to find the following minimizer:

$$W^* = \operatorname{argmin}_W \frac{1}{M} \sum_{i=1}^M L(x_i, y_i; W) + \lambda S(x_i, \epsilon, \nu; W) \quad (9)$$

To evaluate the sensitivity function S during training, any feasible values for the dual variables ν can be used. The optimality of ν affects how conservative the estimated sensitivity will be. For the experiments in the next section, we evaluate S using Algorithm 1 from [21].

6. Experimental Results

In this section, we present two sets of experimental results comparing the performance of our training technique across several metrics against other state-of-art techniques in the literature. The standard handwritten digits data-set MNIST is used in all experiments. The baseline training for all comparisons consists of a cross-entropy loss function with l_2 regularization.

In the first set of experiments, we compare our sensitivity minimization (SM) algorithm against two other techniques which, like the proposed approach, minimize some measure of sensitivity. The first technique [17] (jacobM) performs regularization on the Frobenius norm of the local Jacobian matrix of the network’s classification function, while the second method [43] (specM) implements a regularization scheme on the spectral norm of the network

weights. The results from the first set of experiments are discussed in Sec. 6.1.

The second set of experiments aims at demonstrating that some improvement in performance against adversarial attacks results as a side consequence of sensitivity minimization. To that end, we compare SM against the described baseline approach as well as the algorithm from [21] (K&W), which maximizes an adversarial robustness measure explicitly. The results of these experiments are discussed in Sec. 6.2.

In both experiments, the weight on our sensitivity loss was chosen to be $\lambda = 1 \times 10^{-6}$. This value was empirically optimized based on multiple training runs and provides a good balance between the classification performance and sensitivity of the resulting network. A perturbation bound as described in Sec. 4 with $\sigma = 0.05$ was chosen for all evaluations of sensitivity and adversarial robustness. One training instance with identical sets of mini-batches is executed for each method being tested, and each resulting trained network is evaluated across all metrics under consideration. Performance is measured on both the training and test data. The standard MNIST training and test sets are used throughout.

6.1. Experiments on Sensitivity-Based Optimization

The network architecture consists of two convolutional layers and one fully-connected layer. We use the Adam Optimizer. As stated, the competing training techniques are applied on identical sets of mini-batches. The set of training techniques include SM, specM, jacobM, as well as the baseline. The metrics used to evaluate performance are cross-entropy loss (CE), classification error (ERR), our own sensitivity measure from Eq. 9 (SENSE), the Jacobian loss from [17] (JACOBI), the Spectral loss from [43] (SPECTRAL), and K&W’s [21] adversarial loss (ADV_LOSS) and (ADV_ERR) (i.e., the percentage of the input data for which the application of bounded perturbations could lead to adversarial examples).

The metric values (after convergence) for each of the techniques are listed in Table 1. Top performers are highlighted (dark green), as well as second-best performers that are closer to the top performer than to the bottom performer (lime green). The plots of the evolutions of the metrics through the training process are provided in the appendix.

When compared to the baseline, the results show that the spectral regularization technique has very small impact on the adversarial loss and little to no effect on the adversarial error. Jacobian loss regularization performed better than spectral regularization in terms of those robustness measures; however it still lags behind our sensitivity minimization technique in terms of guaranteeing robustness to adversarial samples. Any increase in robustness once again

Table 1: Performance results on MNIST test data (sensitivity metrics - smaller is better).

Method/Metric	CE	ERR	ADV_LOSS	ADV_ERR
Base	0.033	0.92%	12.12	96.55%
specM	0.034	0.95%	10.31	97.53%
jacobM	0.155	2.74%	2.34	71.73%
SM	0.079	2.26%	0.41	12.62%

Method/Metric	SENSE	JACOB	SPECTRAL
Base.	4.58×10^{12}	17.47	7.19
specM	71.1×10^{12}	12.49	4.17
jacobM	44.5×10^6	2.75	5.07
SM	5.53×10^3	7.75	6.83

Table 2: Performance results on MNIST training data (adversarial metrics - smaller is better)

T/M	CE	ERR	SENSE	ADV_LOSS	ADV_ERR
Base.	0.071	1.94%	1.28×10^{12}	6.25	91.98%
K&W	0.285	8.02%	2.0×10^5	0.55	16.02%
SM	0.138	3.56%	8.76×10^3	0.85	26.36%

comes at the cost of classification performance as both jacobM and SM are behind specM and the baseline in that regard. Our method handily outperforms all competing methods on the adversarial-related metrics.

In terms of the sensitivity measures (i.e., SENSE, JACOB and SPECTRAL), each training method is the best at minimizing its own metric. Regarding the cross-regularizations performance, jacobM outperformed specM by many orders of magnitude at minimizing our sensitivity measure. It is also better than our technique at minimizing the spectral norm. Our technique did perform better than specM at minimizing the Jacobian loss.

6.2. Experiments on Adversarial-Margin-Based Optimization

For the comparison between baseline, SM and K&W, we use a network architecture consisting of one convolutional layer and one fully-connected layer. For this experiment, we used a vanilla stochastic gradient descent (SGD) optimizer without additional heuristics. We compare performance on CE, ERR, SENSE, ADV_LOSS and ADV_ERR.

The final performance numbers for the training and test data are listed in Tables 2 and 3. For more detailed comparisons of how the performance of the techniques on a particular metric evolved through the course of the training, see figures in the appendix.

Our technique outperforms both the baseline and K&W on the sensitivity measure. In terms of the adversarial error, our technique was outperformed by K&W; however, when compared against the baseline, both methods increase the robustness of the network by significant margins. Clearly, there is a correlation between the lower sensitivities and

Table 3: Performance results on MNIST test data (adversarial metrics - smaller is better)

T/M	CE	ERR	SENSE	ADV_LOSS	ADV_ERR
Base	0.082	2.38%	1.27×10^{12}	6.11	91.23%
K&W	0.262	7.3%	2.12×10^5	0.51	14.54%
SM	0.125	3.25%	8.65×10^3	0.79	24.5%

lower adversarial loss/error. While our technique does not minimize the adversarial error directly, the empirical outcome indicated in Table 2 seems to indicate that encouraging small sensitivity has an effect on that measure. Complementarily, the method from [21] directly minimizes the adversarial error by maximizing the adversarial margin; however, as shown in Table 2, it appears to also have significant effect towards minimizing the sensitivity of the network when compared against the baseline.

In terms of classification error and cross-entropy loss, the performance of our training method exceeds that of K&W. We believe this difference in classification performance is due to overfitting in K&W taking place. This could be due to the fact that K&W learns boundaries based on worst-case adversarial examples, which may lead to unnecessarily uneven boundaries, often associated with overfitting; in contrast, our training method reduces the size of the output reachable set uniformly, and not based on any individual sample. The significant gains in classification performance and sensitivity on both training and test sets of our method relative to K&W, more than make up for the comparatively slight loss in adversarial performance.

7. Conclusion and Future Work

In this paper, we studied the relationship between the energy value of optimization landscape minima and the sensitivity and adversarial robustness of the resulting networks. Using formal verification and energy landscape techniques, we empirically showed that there exists a correlation between the sensitivity of a network and the energy value of its corresponding landscape minimum: the lower the energy of the minimum, the less sensitive the network is to perturbations in the input. We also studied the relationship between the sensitivity of a neural network and its adversarial robustness, and show that less sensitive networks tend to be more robust. Furthermore, we found that there is a consistent trade-off between adversarial and sensitivity properties of a network and its classification performance.

Leveraging those experimental findings, we introduced a novel learning framework aimed at optimizing the sensitivity of a network, as measured by the aggregate volume of an over-approximation of the reachable set of network outputs under bounded additive perturbations. We showed experimentally that, as expected, the proposed sensitivity-based learning approach had positive impact on the adversarial ro-

bustness of the resulting networks. Overall, we found that the proposed method compares favorably against state-of-the-art sensitivity-based learning frameworks with regards to adversarial robustness, while at the same time remaining competitive across miscellaneous sensitivity metrics.

An additional set of experiments comparing the performance of the proposed network and an adversarially-tuned state-of-the-art approach showed that application of our method results in a reasonable trade-off between sensitivity, adversarial robustness and classification performance. While the proposed method slightly lagged behind in terms of the computed adversarial metrics, we believe the observed sensitivity gains and ameliorated losses in classification performance represent a more than sensible compromise which may be preferred in certain applications.

References

- [1] <https://pele-python.github.io/pele/>. 6
- [2] P. Baldi and K. Hornik. Neural networks and principal component analysis: Learning from examples without local minima. *Neural networks*, 2(1):53–58, 1989. 3
- [3] A. Ballard, S. Martiniani, D. Mehta, J. Stevenson, and D. J. Wales. Energy landscapes for machine learning. *Phys. Chem. Chem. Phys.*, 19:12585–12603, 2017. 3
- [4] Y. Bengio, I. J. Goodfellow, and A. Courville. Deep learning. *MIT Press.*, 2015. 1
- [5] R. Bunel, I. Turkaslan, P. H. Torr, P. Kohli, and M. P. Kumar. Piecewise linear neural network verification: a comparative study. *arXiv preprint arXiv:1711.00455*, 2017. 3, 4, 5
- [6] C.-H. Cheng, G. Nührenberg, and H. Ruess. Maximum resilience of artificial neural networks. In *International Symposium on Automated Technology for Verification and Analysis*, pages 251–268. Springer, 2017. 3
- [7] A. Choromanska, M. Henaff, M. Mathieu, G. Arous, and Y. LeCun. The loss surfaces of multilayer networks. *arXiv preprint arXiv:1412.0233*, 2014. 3
- [8] S. Dutta, S. Jha, S. Sankaranarayanan, and A. Tiwari. Output range analysis for deep feedforward neural networks. In *NASA Formal Methods Symposium*, pages 121–138. Springer, 2018. 3
- [9] K. Dvijotham, R. Stanforth, S. Goyal, T. A. Mann, and P. Kohli. A dual approach to scalable verification of deep networks. *CoRR*, abs/1803.06567, 2018. 2, 3
- [10] R. Ehlers. Formal verification of piece-wise linear feed-forward neural networks. In *International Symposium on Automated Technology for Verification and Analysis*, pages 269–286. Springer, 2017. 3
- [11] I. Evtimov, K. Eykholt, E. Fernandes, T. Kohno, B. Li, A. Prakash, A. Rahmati, and D. Song. Robust physical-world attacks on deep learning models. *arXiv preprint arXiv:1707.08945*, 1, 2017. 1
- [12] I. Goodfellow, O. Vinyals, and A. Saxe. Qualitatively characterizing neural network optimization problems. *arXiv preprint arXiv:1412.6544*, 2014. 3
- [13] I. J. Goodfellow, J. Shlens, and C. Szegedy. Explaining and harnessing adversarial examples (2014). *arXiv preprint arXiv:1412.6572*. 1
- [14] I. J. Goodfellow, J. Shlens, and C. Szegedy. Explaining and harnessing adversarial examples. *CoRR*, abs/1412.6572, 2014. 3
- [15] S. Gu and L. Rigazio. Towards deep neural network architectures robust to adversarial examples. *CoRR*, abs/1412.5068, 2014. 3
- [16] S. Huang, N. Papernot, I. Goodfellow, Y. Duan, and P. Abbeel. Adversarial attacks on neural network policies. *arXiv preprint arXiv:1702.02284*, 2017. 1
- [17] D. Jakubovitz and R. Giryès. Improving DNN robustness to adversarial attacks using jacobian regularization. *CoRR*, abs/1803.08680, 2018. 3, 7, 11
- [18] G. Katz, C. Barrett, D. L. Dill, K. Julian, and M. J. Kochenderfer. Reluplex: An efficient smt solver for verifying deep neural networks. In *International Conference on Computer Aided Verification*, pages 97–117. Springer, 2017. 2, 3
- [19] K. Kawaguchi. Deep learning without poor local minima. *arXiv preprint arXiv:1605.07110*, 2016. 3
- [20] K. Kawaguchi, L. P. Kaelbling, and Y. Bengio. Generalization in deep learning. *arXiv preprint arXiv:1710.05468*, 2017. 3
- [21] J. Z. Kolter and E. Wong. Provable defenses against adversarial examples via the convex outer adversarial polytope. *arXiv preprint arXiv:1711.00851*, 2017. 2, 3, 5, 7, 8
- [22] A. Kurakin, I. Goodfellow, and S. Bengio. Adversarial examples in the physical world. *arXiv preprint arXiv:1607.02533*, 2016. 1

- [23] D. Mehta, T. Chen, T. Tang, and J. D. Hauenstein. The loss surface of deep linear networks viewed through the algebraic geometry lens. *ArXiv e-prints*, Oct. 2018. 3
- [24] D. Mehta, X. Zhao, E. A. Bernal, and D. J. Wales. Loss surface of xor artificial neural networks. *Phys. Rev. E*, 97:052307, May 2018. 3
- [25] Q. Nguyen and M. Hein. The loss surface of deep and wide neural networks. *arXiv preprint arXiv:1704.08045*, 2017. 3
- [26] R. Novak, Y. Bahri, D. A. Abolafia, J. Pennington, and J. Sohl-Dickstein. Sensitivity and generalization in neural networks: an empirical study. In *International Conference on Learning Representations*, 2018. 3
- [27] G. Optimization. Inc.,gurobi optimizer reference manual, 2015. URL: <http://www.gurobi.com>, 2014. 4
- [28] N. Papernot, N. Carlini, I. Goodfellow, R. Feinman, F. Faghri, A. Matyasko, K. Hambardzumyan, Y.-L. Juang, A. Kurakin, R. Sheatsley, et al. cleverhans v2.0.0: an adversarial machine learning library. *arXiv preprint arXiv:1610.00768*, 2016. 1
- [29] D. Peled. *Software Reliability Methods*. Texts in Computer Science. Springer, 2001. 3
- [30] L. Pulina and A. Tacchella. Challenging smt solvers to verify neural networks. *AI Commun.*, 25:117–135, 2012. 3
- [31] A. Richards and J. How. Mixed-integer programming for control. In *American Control Conference, 2005. Proceedings of the 2005*, pages 2676–2683. IEEE, 2005. 4
- [32] A. Saxe, J. McClelland, and S. Ganguli. Exact solutions to the nonlinear dynamics of learning in deep linear neural networks. *arXiv preprint arXiv:1312.6120*, 2013. 3
- [33] J. Sokolic, R. Giryes, G. Sapiro, and M. R. D. Rodrigues. Robust large margin deep neural networks. *IEEE Transactions on Signal Processing*, 65:4265–4280, 2017. 3
- [34] L. Song and P. Mittal. Inaudible voice commands. *arXiv preprint arXiv:1708.07238*, 2017. 1
- [35] D. Soudry and Y. Carmon. No bad local minima: Data independent training error guarantees for multilayer neural networks. *arXiv preprint arXiv:1605.08361*, 2016. 3
- [36] C. Szegedy, W. Zaremba, I. Sutskever, J. Bruna, D. Erhan, I. Goodfellow, and R. Fergus. Intriguing properties of neural networks. *arXiv preprint arXiv:1312.6199*, 2013. 1
- [37] A. Taghvaei, J. W. Kim, and P. Mehta. How regularization affects the critical points in linear networks. In I. Guyon, U. V. Luxburg, S. Bengio, H. Wallach, R. Fergus, S. Vishwanathan, and R. Garnett, editors, *Advances in Neural Information Processing Systems 30*, pages 2502–2512. Curran Associates, Inc., 2017. 3
- [38] Theano Development Team. Theano: A Python framework for fast computation of mathematical expressions. *arXiv e-prints*, abs/1605.02688, May 2016. 6
- [39] D. J. Wales. *Energy Landscapes*. Cambridge University Press, Cambridge, 2003. 5
- [40] D. J. Wales. Some further applications of discrete path sampling to cluster isomerization. *Mol. Phys.*, 102:891–908, 2004. 3
- [41] L. Wu, Z. Zhu, and W. E. Towards Understanding Generalization of Deep Learning: Perspective of Loss Landscapes. *ArXiv e-prints*, June 2017. 3
- [42] H. Xu and S. Mannor. Robustness and generalization. *CoRR*, abs/1005.2243, 2010. 2
- [43] Y. Yoshida and T. Miyato. Spectral norm regularization for improving the generalizability of deep learning. *CoRR*, abs/1705.10941, 2017. 3, 7

A. Appendix - Section 6: Experimental Results

The plots included in this appendix illustrate the evolution of the different losses through the training process of the methods being compared.

A.1. Experiments on Sensitivity-Based Optimization (Sec. 6.1)

Note that the shifts in behavior observed in the plots describing the evolution of jacobM [17] are due to the fact that the method consists of three separate training stages: between epochs 1 and 41, it is equivalent to the baseline method; between epochs 41 and 59, it incorporates dropout on top of the baseline approach; lastly, from epoch 61 on, it enforces the Jacobian loss term.

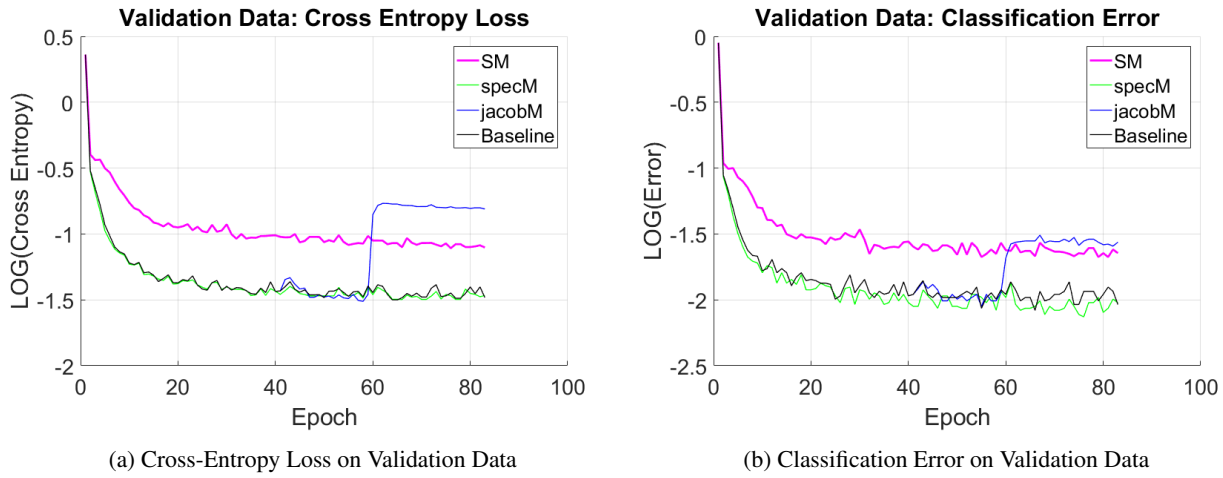


Figure 8: Performance Comparison - Performance Metrics

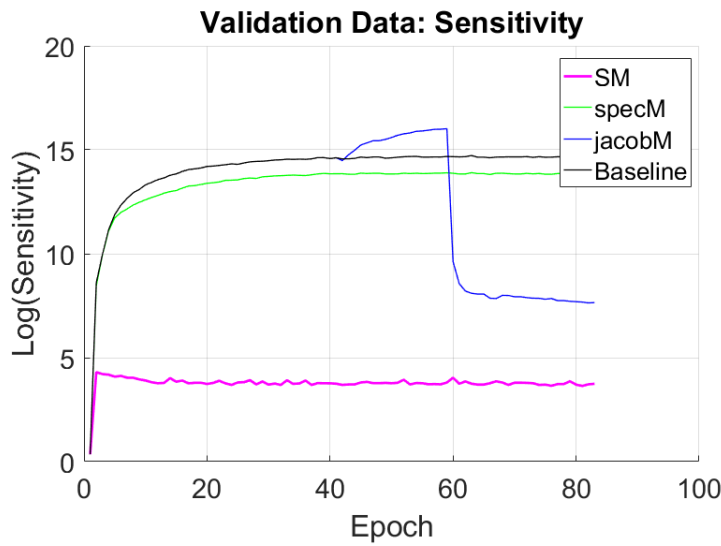
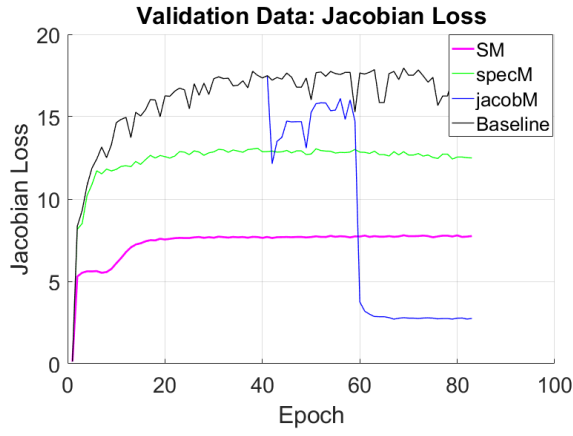
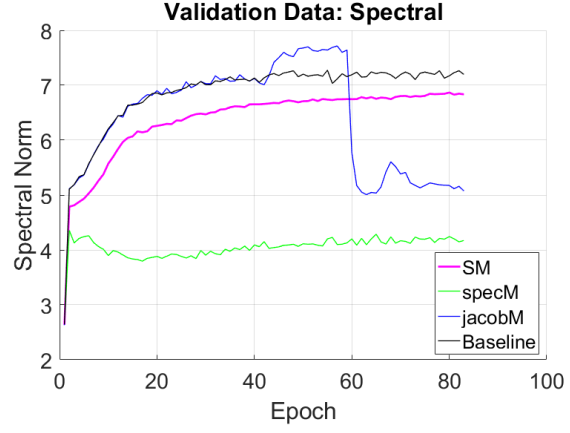


Figure 9: Sensitivity on Validation Data



(a) Jacobian Loss on Validation Data

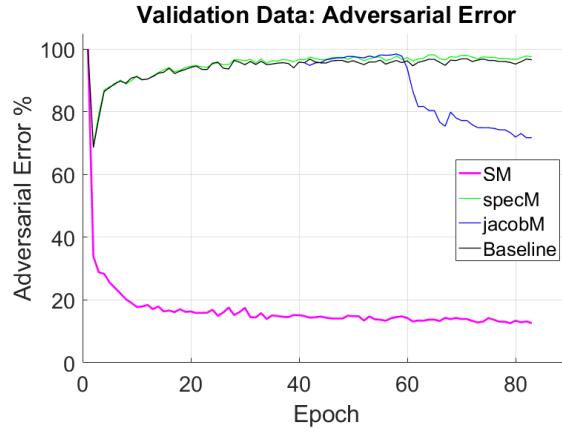


(b) Spectral Loss on Validation Data

Figure 10: Performance Comparison - Other Sensitivity Metrics



(a) Adversarial Loss on Validation Data

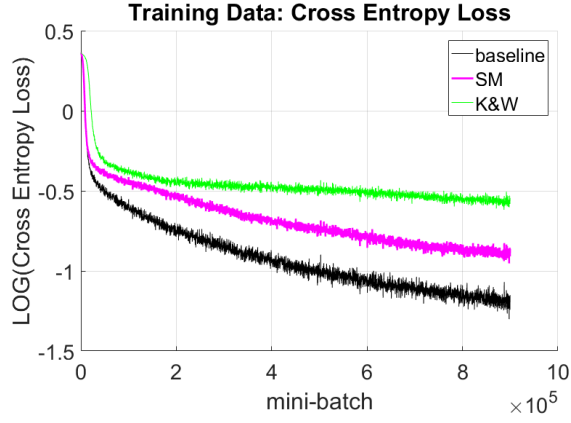


(b) Adversarial Error on Validation Data

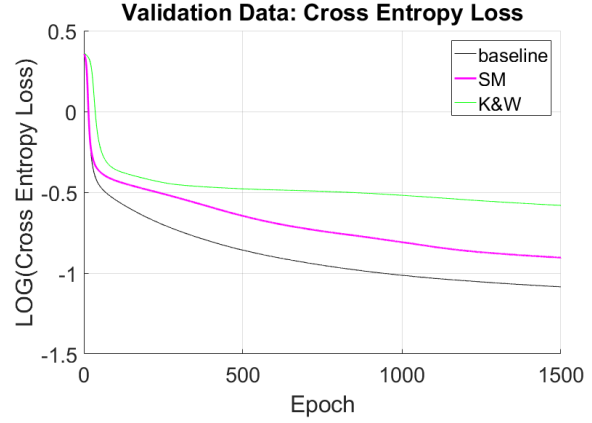
Figure 11: Performance Comparison - Adversarial Metrics

A.2. Experiments on Adversarial-Margin-Based Optimization (Sec. 6.2)

Note that the granularity of all training data plots is 250 mini-batches.

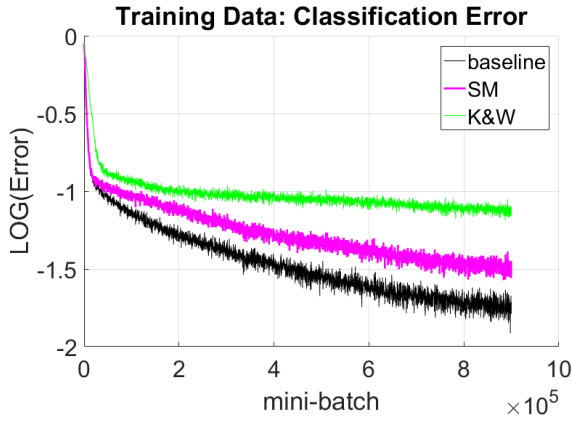


(a) Cross-Entropy Loss on Training Data

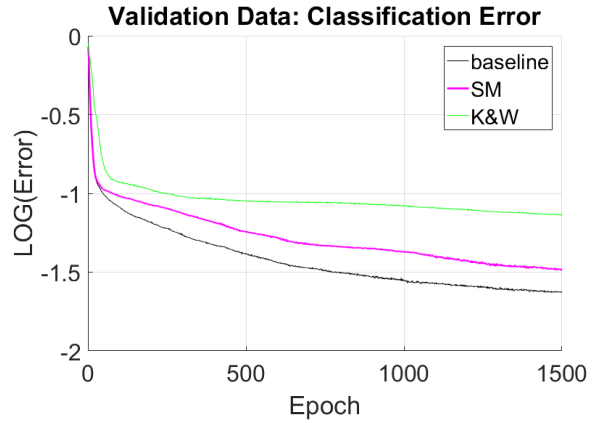


(b) Cross-Entropy Loss on Validation Data

Figure 12: Performance Comparison - Cross-Entropy Loss

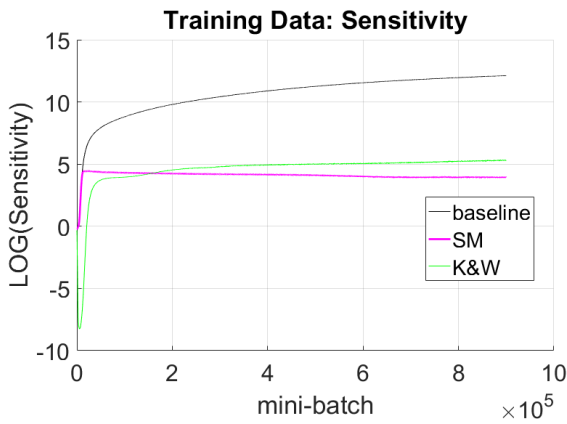


(a) Classification Error on Training Data

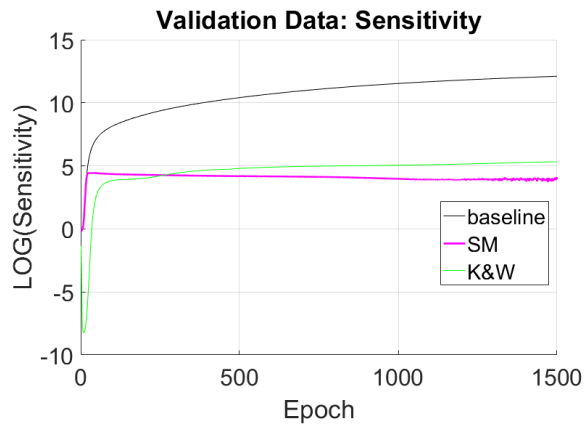


(b) Classification Error on Validation Data

Figure 13: Performance Comparison - Classification Error Rate

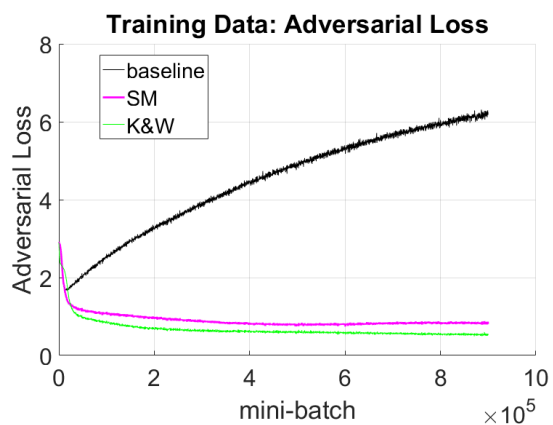


(a) Sensitivity on Training Data

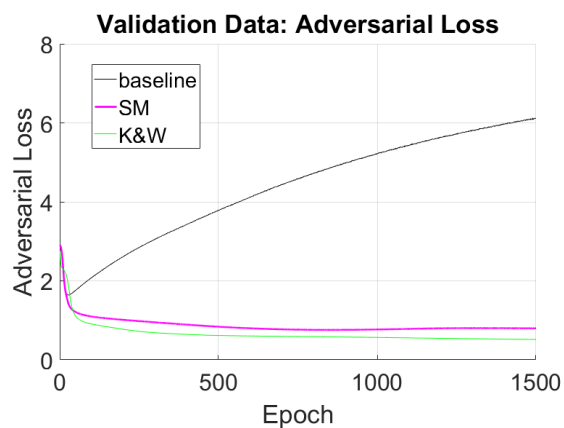


(b) Sensitivity on Validation Data

Figure 14: Performance Comparison - Sensitivity

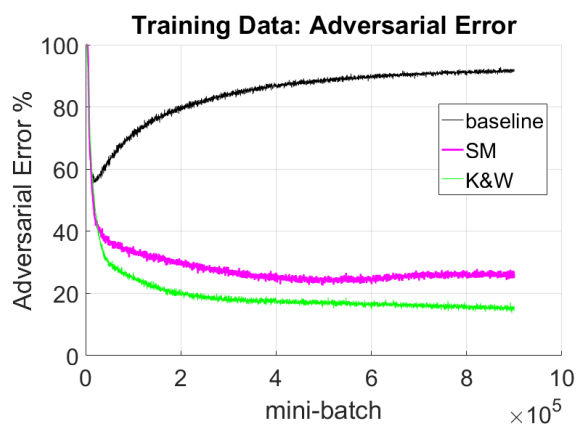


(a) Adversarial Loss on Training Data

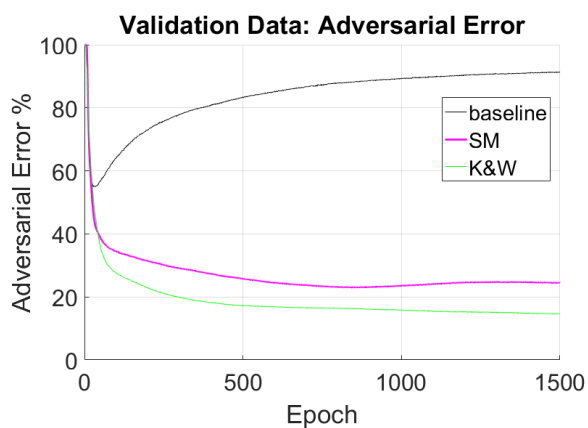


(b) Adversarial Loss on Validation Data

Figure 15: Performance Comparison - Adversarial Loss



(a) Adversarial Error Rate on Training Data



(b) Adversarial Error Rate on Validation Data

Figure 16: Performance Comparison - Adversarial Error Rate